LAWRENCE
LIVERMORE
NATIONAL
LABORATORY

UCRL-JRNL-231035

Geometrical Effects in Plasma Stability and Dynamics of Coherent Structures in the Divertor

D. D. Ryutov, R. H. Cohen

May 18, 2007

Contributions to Plasma Physics

Geometrical effects in plasma stability and dynamics of coherent structures in the divertor

D.D. Ryutov*, R.H. Cohen

Lawrence Livermore National Laboratory, Livermore, CA 94551, USA

Abstract

Plasma dynamics in the divertor region is strongly affected by a variety of phenomena associated with the magnetic field geometry and the shape of the divertor plates. One of the most universal effects is the squeezing of a normal cross-section of a thin magnetic flux-tube on its way from the divertor plate to the main SOL. It leads to decoupling of the most unstable perturbations in the divertor legs from those in the main SOL. For perturbations on either side of the X-point, this effect can be cast as a boundary condition at some "control surface" situated near the X-point. We discuss several boundary conditions proposed thus far and assess the influence of the magnetic field geometry on them. Another set of geometrical effects is related to the transformation of a flux-tube that occurs when it is displaced in such a way that its central magnetic field line coincides with some other field line, and the magnetic field is not perturbed. These flute-like displacements are of a particular interest for the low-beta edge plasmas. It turns out that this transformation may also lead to a considerable deformation of a flux-tube cross-section; in addition, the distance between plasma particles occupying the flux-tube may change significantly even if there is no parallel plasma motion. We present expressions describing aforementioned transformations for the general tokamak geometry and simplify them for the divertor region (using the proximity of the X-point). We also discuss the effects associated with the shape of the plasma-limiting surfaces, both those designed to intercept the plasma (like divertor plates and limiters) and those that can be hit in some "abnormal" events, e.g., in the course of a radial motion of an isolated plasma filament. The orientation of the limiting surface with respect to the magnetic field affects the plasma dynamics via the sheath boundary conditions. One can enhance or suppress plasma instabilities in the divertor legs by tilting the divertor plate with respect to the poloidal magnetic field. We concentrate on the instabilities in the private flux region and provide stability criteria accounting for the real divertor geometry, going beyond the slab approximation used before.

1 Introduction

Plasma dynamics in the divertor region is strongly influenced by a variety of effects associated with the magnetic field geometry and the shape of the divertor plates. One of the most universal effects is the squeezing of a normal cross-section of a thin magnetic flux-tube on its way from the divertor plate to the main SOL [1] (or from one divertor plate to another in the private flux region). The other effect is associated with the tilt of the divertor plates with respect to the poloidal magnetic field: depending on the tilt, the instabilities of the divertor plasma can be made stronger or weaker [2]. In this paper we consider both effects for the X-point divertor geometry, as shown in Fig. 1. We discuss two aspects of these effects: first, their role in the linear stability analysis of the divertor plasma; second, in their effect on the isolated coherent filamentary structures (often time called "blobs" after paper [3]).

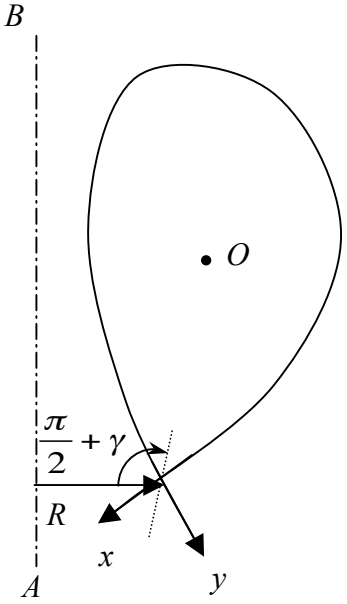

Fig. 1 The shape of the separatix. *AB* is a major axis, *O* is the magnetic axis, R is the major radius of the X point. The dotted line represents a bisector of an angle formed by two branches of a separatrix in the X point. The angle γ is the angle between the bisector and the major axis. Note that in tokamaks with a high triangularity this angle may be close to $\pi/2$, meaning that the inner divertor leg is almost parallel to the major radius, whereas the outer leg is almost perpendicular to it.

In the past, both problems of the divertor stability and dynamics of blobs has received a considerable attention. The linear plasma stability in the divertor legs has been considered in many details (see Refs. [4,5] and references

* Corresponding author: ryutov1@llnl.gov

therein). The main problem in the stability analysis is the proper accounting for the shearing of perturbations in the vicinity of the X-point. This has been done by encapsulating the shearing effect into the boundary conditions applied at some "control" surface situated near the X-point. The basic observation was that, in the region where perturbations become strongly jagged, cross-field current is formed, and the presence of the finite parallel resistivity leads to decay of the potential perturbations along the field lines. Specific mechanisms of the cross-field current formation included ion viscosity [5], electron cross-field resistivity [4] (acting in the zone that the cross-field scale becomes smaller than the ion gyro-radius), and the ion polarization current [7-9]. In the present article, we provide a solution of the stability problem for the X-point geometry with a quantitative description of the magnetic shearing effects in a low-beta plasma. We observe details of disconnection process and provide a quantitative description of various unstable modes. We go beyond the usually used slab approximation and clarify constraints on the applicability of heuristic boundary conditions [4].

In the area of the blob dynamics, we consider the behavior of an "isolated" blob, meaning by that a plasma filament whose density is much higher than the ambient density. Such objects have been experimentally observed in the outer scrape-off layer of tokamaks [10-12]. Our primary interest will be in studying the blobs in the vicinity of the X-point. Here we apply a technique for isolating the global motion of the blob described in Ref. [13]. We produce convenient and easy-to-use results describing the blob dynamics in the case where the filament extends from the zone above the X-point to the zone below the X-point. We consider also the situation where the filament is terminated by a material surface in the main plasma chamber. The surface may be that of a deliberately introduced limiter, or a piece of equipment, like the RF antenna. The effect of this contact depends on the location and the tilt of the surface. We discuss also effects of a plasma redistribution along the moving filament.

The linear stability analysis is discussed in Sec. 2, whereas the blob dynamics in Sec. 3. Sec. 4 contains the summary of our findings. Some more lengthy calculations are presented in Appendices 1 and 2.

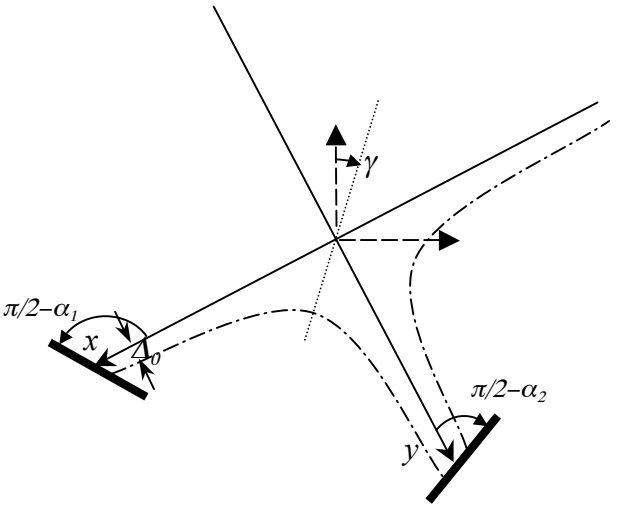

Fig. 2 The vicinity of the X-point. Dash-dotted lines represent two field lines (projected onto poloidal plane). Thick lines represent diverotr plates. The dotted line is a bisector of the angle formed by two branches of the separatrix.

2 Linear plasma stability in the divertor

2.1 The geometry of the problem and plasma model

The typical shape of a separatrix is shown in Fig. 1. We will be interested in analyzing the area in the vicinity of the X-point, which is shown in more detail in Fig. 2. The separatrix here can be presented as an orthogonal intersection of two straight lines. We orient the Cartesian coordinate axes along these lines, as shown in Fig. 2. The quadrant $x>0$, $y>0$ corresponds to the private flux region. The coordinate z (an analog of the toroidal coordinate) is directed towards the viewer.

The poloidal magnetic field in the vicinity of the X point can be presented as $B_x = const \times x$, $B_y = -const \times y$, with the same constant in both cases. We will relate this constant to the magnitude of the poloidal field $B_P>0$ in the vicinity of the divertor plate, i.e., at $x=l_d$, y=0, with l_d being the distance between the X point and the divertor plate. In other words, we have

$$B_x = B_P x / l_d,\ B_y = -B_P y / l_d. \qquad (1)$$

Clearly, we assume that l_d is significantly less than the plasma minor radius, and the major radius of the X-point. Wherever possible, we neglect the terms of order l_d/R (retaining them only when assessing the curvature drive). In particular, when characterizing the field lines in the vicinity of the X point, we assume that the toroidal field is uniform, $B_z=B_T>0$. Then, one can easily show that the equation of the field line starting at the point (x_0, y_0, z_0) is (Cf. [1]):

$$x = x_0 e^{(z-z_0)/L};\ y = y_0 e^{-(z-z_0)/L} \qquad (2)$$

where $L=B_T l_d/B_P$. Note that $xy=x_0y_0$. We assume that in the divertor region $B_P<<B_T$. The scrape-off layer (SOL) thickness Δ_0 in the strike point (Fig. 2) is assumed to be much smaller than the length l_d of the divertor legs. Dash-dotted lines in Fig. 2 depict field lines passing at the distance Δ from the separatrix at the strike points.

A fluxtube that has a circular crossection in some toroidal location $z=z_0$, becomes an ellips whose major semi-axis is

$$e^{(z-z_0)/L} \equiv E \tag{3}$$

times larger than the initial radius [1]; the minor semi-axis becomes by a factor of E smaller than the initial radius. We call the parameter E "elongation". The squeezing is the manifestation of the magnetic shear effect (Cf. Ref. [1]).

The orientation of the divertor plates with respect to the poloidal field in the strike points can be characterized by the angles α_1 and α_2 (Fig. 2). The sign convention corresponds to the situation where positive values of α_1 and α_2 correspond to the situation where the "wetted" surfaces are facing the private flux region (in particular, in Fig. 2 $\alpha_1>0$, $\alpha_2<0$). The intersection of the divertor plates with the separatrix is assumed to be not too shallow, $\Delta/|\cos\alpha_{1,2}|<< l_d$.

With regard to the plasma properties in the unperturbed state, we assume the simple model used in a number of earlier studies of the divertor-leg instabilities [4,5,14]: all the plasma parameters are uniform, except for the electron temperature T_e, which varies across the flux surfaces. Thereby, we retain only the drive associated with the gradient of T_e , neglecting the drive associated with the density and the ion temperature gradients. A justification for this model (aside from the convenience of comparing our results with the earlier work) is that the cross-field gradient of the electron temperature in the SOL is typically steeper than that of the density and the ion temperature (regarding which we assume that it is of the same order as T_e). As the plasma potential (with respect to divertor plates, which we assume are grounded) is roughly proportional to T_e, there is also the electrostatic potential variation across the flux surfaces, and, therefore, the EXB drift in the unperturbed state. The drift velocity is predominantly poloidal.

2.2 Basic equations

Instability that is studied in the present paper is of the type discussed in Refs. [2, 5, 15, 16], which can be described within MHD model in terms of the bulk plasma motion and complemented by the boundary conditions relating the plasma displacement and the current on the plasma side of the sheath at the divertor plate. Typical growth rate of this instability is much shorter than the ion transit time between the X-point and the divertor leg. Therefore, the ion thermal spread is unimportant; it is also unimportant whether the ion mean free path is shorter or longer than the connection length $L_{||}$ between the control surface and the divertor plane: the ions enter the problem just via their cross-field inertia. With regard to electrons, we assume that their collision frequency is higher than the growth rate. Under such conditions, the momentum equation can be presented as:

$$m_i n \delta \frac{d\mathbf{v}}{dt} = -\nabla \delta p + \frac{\delta \boldsymbol{j}_\perp \times \boldsymbol{B}}{c} + m_i n \nu \nabla \cdot \delta \mathbf{v} \tag{4}$$

where ν is the kinematic viscosity. Why we have retained a (small) viscosity? The pressure perturbation is $\delta p = n\delta T_e$, as the plasma density and the ion temperature are assumed to be uniform in the unperturbed state. The electron temperature perturbation can be found from equation

$$\delta \dot{T}_e = -\delta \mathbf{v} \cdot \nabla T_{eo} \tag{5}$$

For a low-beta plasma, we will consider only the modes that do not perturb the magnetic field (the finite-beta effects have been considered in a slab geometry in Ref. CR-PPCF). Then, the electric field perturbation can be described as an electrostatic perturbation, with the parallel component of the electric field related to the finite plasma resistivity (allowing thereby for the resistive ballooning [13]). The velocity perturbation is directed across the magnetic field:

$$\delta \mathbf{v} = c \frac{\boldsymbol{B} \times \nabla \delta\varphi}{B^2} \tag{6}$$

The potential perturbation varies slowly along the field lines compared to the variation in the transverse direction. It is convenient to describe it using the coordinates (x_0, y_0) of the foot-point of the field line at the divertor plate, and the coordinate z (which, up to the small terms of order of B_P/B_T coincides with the field line): $\delta\varphi = \delta\varphi(x_0, y_0, z)$. We consider an instability with the length scale of perturbations in the direction normal to the flux surfaces small compared to the characteristic SOL thickness. This allows one to use an eikonal approximation

$$\delta\varphi = \delta\varphi_0(z) \exp\left(-i\omega t + ik_{0x}x_0 + ik_{0y}y_0\right) \tag{7}$$

As there is an unperturbed electric field directed along the normal to the flux surface, there exists an unperturbed drift velocity with the component lying within the flux surface. This leads to that the operator d/dt, when applied to perturbations of the type (7), becomes $d/dt \to -i\Omega$, $\Omega = \omega - \boldsymbol{k}_0 \mathbf{v}_{D0}$, where $\mathbf{v}_{D0}$ is the unperturbed drift velocity near the divertor plate.

Using the current continuity equation, with $\delta \boldsymbol{j}_\perp$ determined from Eq. (4), one finds that

$$\frac{\partial j_\parallel}{\partial z} = \frac{2c}{RB}\boldsymbol{b}\cdot\nabla\delta p + \frac{m_i n c^2}{B^2}\left[i\Omega\nabla_\perp^2\delta\varphi + \nu\nabla_\perp^2(\nabla_\perp^2\delta\varphi)\right] \tag{8}$$

where R is a major radius in the vicinity of the X-point. We consider it as a constant, which is sufficient if we do not depart too strongly from the X-point. We have also consistently used the smallness of the parameter B_P/B_T (which is indeed quite small near the X point).

The pressure perturbation can be found from Eqs. (5), (6), with the account for the fact that the unperturbed temperature is constant over flux surfaces, i.e., $T_e = T_e(\Phi)$, $\Phi = (B_P/l_d)xy$:

$$\delta p = \pm\frac{icn}{\Omega B}\frac{T_e}{\Delta_0 l_d}\left(y\frac{\partial\delta\varphi}{\partial y} - x\frac{\partial\delta\varphi}{\partial x}\right) \tag{9}$$

$$\frac{T_e}{\Delta_0} = \pm B_P\frac{\partial T_e}{\partial\Phi} \tag{10}$$

An equation for the parallel current is:

$$\delta j_\parallel = -\frac{1}{\eta}\frac{\partial\delta\varphi}{\partial z} \tag{11}$$

Equations (8), (9), (11) form a complete set that determines the spatial structure of the potential perturbations.

For the potential perturbation of the form (7), one obtains (by using Eqs. (2) and (3)):

$$\nabla_\perp^2\delta\varphi = -\left(k_{x0}^2E^2 + k_{y0}^2E^{-2}\right)\delta\varphi \tag{12}$$

and

$$\delta p = \pm\frac{icn}{\Omega B}\frac{T_e}{\Delta_0 l_d}\left[y_0k_{0y} - x_0k_{0x}\right]\delta\varphi \tag{13}$$

2.3 Flute perturbations.

Before introducing general sheath BC, we consider an important auxiliary problem of pure flute perturbations. The ideal flute instability corresponds to a zero plasma viscosity, zero electrical resistivity, and non-conducting end-plates ($j_\parallel$=0 at both plates). The electrostatic potential perturbation is constant along the field line, i.e., the dependence of $\delta\varphi_0$ on z in () should be suppressed. The drive for the flute instability is predominantly situated in the inner leg, where the projection of the pressure gradient on the curvature radius is large. One may naively think that the presence of the other leg makes a stabilizing contribution but, as we see, this is not the case.

Substituting the pressure perturbation (13) into Eq. (8), using Eqs. (2) and (12), setting $\delta\varphi_0$=const, and integrating Eq. (12) between the divertor plates, one obtains the following dispersion relation:

$$\Omega^2\int\left(k_{x0}^2E^2 + k_{y0}^2E^{-2}\right)dz = \frac{2T_e}{m_iR\Delta_0 l_d}\left(y_0k_{0y} - x_0k_{0x}\right)\int\left[\cos\left(\frac{\pi}{4}+\gamma\right)k_{x0}E + \cos\left(\frac{\pi}{4}-\gamma\right)\frac{k_{y0}}{E}\right]dz \tag{14}$$

We have written this equation for the instability in the private flux region, with the sign convention corresponding to the geometry of Fig. 2. The initial point in the integration is situated at the inner plate, whereas the final point is situated at the outer plate. Accordingly, we start from E=1, and end up with some $E=E^*>1$ that corresponds to the elongation at the outer strike point. We ignore effect of tilt of the divertor plates assuming that $\alpha_1=\alpha_2=0$ (we will add this effect later, in a more general analysis). Note that the term proportional to k_{x0} in the integrand (which is the main driving term) does not change sign between the inner and outer leg.

Noting that, according to Eq. (3), $dz = LdE/E$, one can rewrite Eq. (14) in a more convenient way:

$$\frac{\Omega^2}{2}\left[k_{x0}^2\left(E^{*2}-1\right) + k_{y0}^2\left(1-E^{*-2}\right)\right] = \frac{2T_e}{m_iR\Delta_0 l_d}\left[\cos\left(\frac{\pi}{4}+\gamma\right)k_{x0}\left(E^*-1\right) + \cos\left(\frac{\pi}{4}-\gamma\right)k_{y0}\left(1-E^{*-1}\right)\right]\left(y_0k_{0y} - x_0k_{0x}\right) \tag{15}$$

This expression is valid for both "short" and "long" divertor legs, i.e., for both $l_d \sim \Delta_0$, and $l_d >> \Delta_0$. Note that in the latter case the inertia scales as E^{*2} due to a large x component of the displacement in the outer leg (where E>>1). In

Eq. (15) we do not assume the equal length of the divertor legs, i.e., it is quite general. For long divertor legs, $l_d >> \Delta_0$, one has $x_0 \approx l_d$, $y_0 \approx \Delta_0$, $E^* \approx l_d/\Delta_0 >> 1$, so that

$$\Omega^2 = -\frac{4T_e}{m_i R \Delta_0 E^*} \cos\left(\frac{\pi}{4} + \gamma\right) \tag{16}$$

Note the appearance of the small parameter $1/\sqrt{E^*}$ in the growth rate $\Gamma \equiv \mathrm{Im}\Omega$ of the instability.

2.4 Resistive ballooning and the ion gyroradius cut-off

We now consider the possible modification of the flute instability in the presence of finite plasma resistivity. We approach this problem by formulating conditions under which the potential variation along the fluxtube becomes significant.

At a finite plasma resistivity, the potential perturbation will no more be constant along the field line. The contribution to the parallel current density (which, at a finite resistivity, is a measure of the potential variation) arises predominantly from the terms in square brackets in Eq. (8), because these terms scale as a high power of E and increase dramatically on the way from the inner to the outer divertor leg. So, the potential perturbations may decrease substantially in the outer leg, thereby meaning the appearance of the modes localized in the inner leg. Although we have neglected the viscous terms in the analysis of the previous section, we retain them here, as they grow as E^4 and may become significant in the decoupling. The plasma resistivity *per se* , under conditions of tokamak divertor, is usually not sufficient to cause significant ballooning. Here it is enhanced by the presence of large multipliers proportional to the powers of E. Accordingly, the effects of resistive ballooning are enhanced in divertors with long legs.

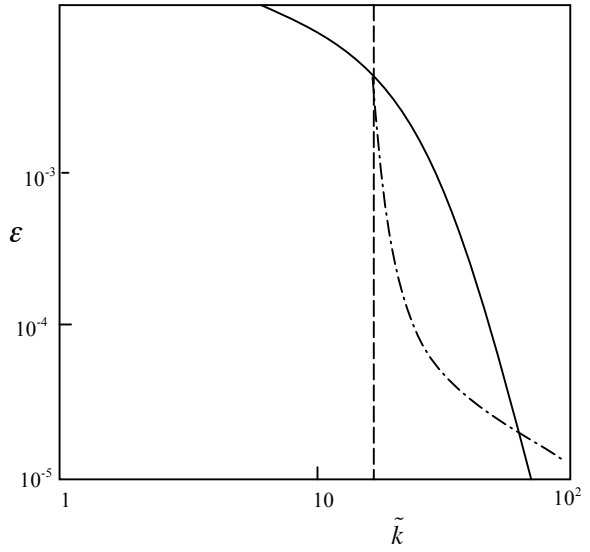

Fig. 3 On the problem of resistive ballooning. The dash-dotted line depicts the condition where resistive ballooning occurs due to the cross-field current leaks in the regime where the wave number becomes higher than inverse ion gyro-radius. Above this line the heuristic BC of Ref. [4] can be applied. Other explanations are given in the text.

Substituting a constant (along the field lines) potential $\delta\varphi_0$ into the terms in the square brackets in Eq. (8) and integrating them from one plate to another using the relationship $dz = LdE/E$, one finds the resistive potential variation $\delta\varphi_1$:

$$\left|\frac{\delta\varphi_1}{\delta\varphi_0}\right| \sim \frac{D_M L^2}{v_A^2 \Delta_0^2 \Gamma_0}\left[\left|\frac{\Omega}{\Gamma_0}\right|\tilde{k}^2 + \frac{\nu}{\Gamma_0 \Delta_0^2}\tilde{k}^4\right] \tag{17}$$

where $\tilde{k}$ is the dimensionless wave number $\tilde{k} \equiv k_{x0}\Delta_0 E$, Γ_0 is a growth-rate of the curvature-driven instability without shearing factors included,

$$\Gamma_0 \equiv \frac{c_S}{\sqrt{R\Delta_0}}, \tag{18}$$

and $D_M \equiv c^2\eta/4\pi$ is the magnetic diffusivity. Consider the numerical value of the coefficient in front of the square bracket for the following set of plasma parameters (Cf. Sec. 3 of Ref. 5): $T_e \sim T_i \sim 25$ eV, $n \sim 10^{13}$ cm^{-3}, R~ 50 cm, L~ 300 cm, Δ_0~ 1cm, and B~ 5 T. These parameters correspond to the parameters of a compact high-field tokamak, although in real machine each of them can vary by a factor of a few. For this set of parameters, the coefficient in front

of the square bracket is quite small, ~ 10^{-4}. In other words, the resistive disconnection between the plates may occur only at large elongations and/or high wave numbers. The dimensionless parameter in front of the second term in the square bracket is also small, of order of 10^{-3}. However, the second term may still become dominant for large E and k.

These results are illustrated with Fig. 3, where the parameter space is represented in the k-ε plane, where

$$\varepsilon \equiv \frac{D_M L^2}{v_A^2 \Delta_0^2 \Gamma_0} \tag{19}$$

The solid line represents the condition where the l.h.s. of Eq. 1 is equal to one. Below this line, resistive ballooning is unimportant, whereas above this line it is significant. When plotting this line we assumed that the parameter

$$\mu \equiv \frac{\nu}{\Gamma_0 \Delta_0^2} \tag{20}$$

is 10^{-3}. The dashed line represents the condition where the wave number at the outer plate becomes (formally) higher than the inverse ion gyroradius, under the assumption that parameter Δ_0/ρ_i=20. Our description has to be modified to the right of this line.

$$E = \frac{1}{k_{x0}\rho_i} \tag{21}$$

In the zone between this point and the outer divertor plate the ions do not participate in the drift motion described by Eq. (6); their cross-field velocity becomes much less than (6).

We concentrated on the flute-type instability. Other instabilities [15, 16] depending on the sheath boundary conditions [17-19] can be also included into analysis.

3. Geometrical effects in the dynamics of isolated blobs.

3.1 Blobs in the framework of an ideal magnetohydrodynamics

In this section we consider the global motion of isolated filament in the divertor region, both in the private and the common flux region, in the MHD approximation. In the case of a perfectly conducting, zero beta plasma, the only type of displacement allowed is the displacement for which the fluxtube in its new location coincides with some magnetic flux tube (Cf. [13]). We concentrate on the dynamics of isolated filaments in the vicinity of the X-point, both in the common and the private flux region and we use a simple model of the magnetic field lines described by Eqs. (2), (3). Numerous other aspects of the blob dynamics have been studied in Refs. [20-28].

We characterize the initial position of the flux tube by the coordinates of its end point (x_0, y_0), and its displacement by the vector $\boldsymbol{\xi}_0=(\xi_{0x}\ \xi_{0y})$ see Fig. 3. In the divertor region, this way of characterization of the displacement is more convenient than the more general way (based on the use of the normal and geodesical displacements) used in Ref. [13] in a general toroidal geometry. Applying Eqs. (15) of Ref. (13), and retaining only the leading order terms in the parameter $B_p/B_T<<1$, one finds:

$$\ddot{\xi}_{0x} = -\frac{2p\cos\left(\frac{\pi}{4}-\gamma\right)}{\rho R}\frac{E\ln E}{E-1};\quad \ddot{\xi}_{0y} = \frac{2p\cos\left(\frac{\pi}{4}+\gamma\right)}{\rho R}\frac{\ln E}{E-1}, \tag{22}$$

where $E = y_1 / y_0 > 1$. The signs correspond to the geometry of Fig. 4. For brevity, we consider the plasma pressure and the density as constant over the flux tube (although the general case can also be easily assessed). The elongation enters the problem via Eqs. (2) – (3). The displacement of the other end of the filament is: $\xi_{1x} = \xi_{0x} E$, $\xi_{1y} = \xi_{0y} / E$. Note that, for the fluxtube extending well into the divertor area, the displacement is predominantly poloidal, with one end of the filament moving "up", and the other moving "down". The normal motion is much slower. Can be extended (qualitatively) up to the blobs reaching the equatorial plane of a tokamak. For reference purpose, we present here a relation between the (ξ_x, ξ_y) component of the displacement and the normal and poloidal components (ξ_n, ξ_p):

$$\xi_n = \frac{\xi_x y - \xi_y x}{\sqrt{x^2 + y^2}}; \quad \xi_p = \frac{\xi_x x + \xi_y y}{\sqrt{x^2 + y^2}} \qquad (23)$$

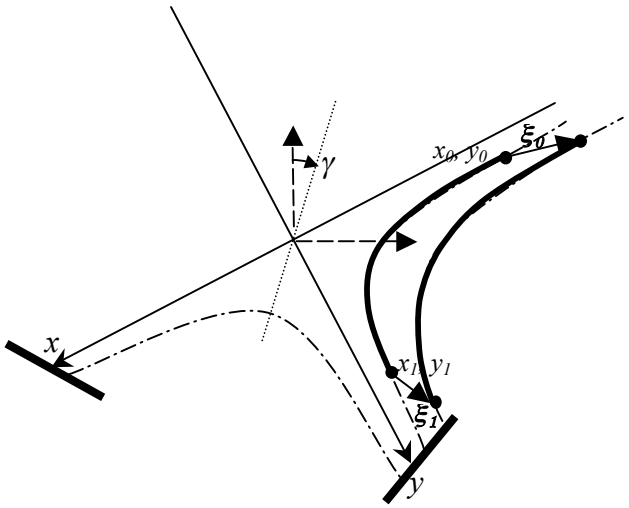

Fig. 4. The projection of the filament onto poloidal plane. The end point of the filament in the main SOL is (x_0, y_0), whereas the other end point (which can be situated both above and below the X point) is (x_1, y_1). For clarity, the end-points are shown by large dots. The filament in its new position is situated further from the separatrix. The end points are displaced by the vectors $\boldsymbol{\xi}_0$ and $\boldsymbol{\xi}_1$, respectively.

Also helpful are expression relating the normal and poloidal displacement in an arbitrary point vs. the displacement in the reference ("0") point:

$$\xi_n = \xi_{n0} \frac{\sqrt{x_0^2 + y_0^2}}{\sqrt{E^2 x_0^2 + y_0^2 / E^2}}; \quad \xi_t = \xi_{t0} \frac{\sqrt{E^2 x_0^2 + y_0^2 / E^2}}{\sqrt{x_0^2 + y_0^2}} + \xi_{n0} \frac{x_0 y_0 \left(E^2 - 1/E^2\right)}{\sqrt{x_0^2 + y_0^2}\sqrt{E^2 x_0^2 + y_0^2 / E^2}} \qquad (24)$$

3.2 Blobs in contact with the divertor plate.

If the blob radius a in the main SOL (at the upper end in Fig. 3) is sufficiently large, then, even with the account of the shear squeezing, the minor semi-axis of the blob near the divertor plate, a/E, may remain larger than the ion gyro-radius, and the macroscopic description would remain valid over the whole blob length. The corresponding condition reads as $a / E > \rho_i$, or as

$$a y_0 > \rho_i y_1. \qquad (25)$$

Previously, in Refs. [5, 19] the situation where this condition is violated by a large margin was considered. Here we assess the opposite case, which corresponds to the blob of a not-too-small cross-section and/or divertor with not too long legs.

The presence of the contact with the wall slows down the blob motion and leads to the situation where the acceleration becomes small, and the motion at a constant velocity takes over. The technique for accounting for the effect of sheath boundary condition on the global motion was presented in Sec. VI of Ref. [13], where the filament in contact with a toroidal limier was considered. In the case of a poloidal divertor the geometry is quite different and some rework of the derivation of Ref. [13] is needed. The boundary condition at the wall is:

$$\frac{c}{B}\left(\frac{\partial p}{\partial x}\cos\alpha_2 - \frac{\partial p}{\partial y}\sin\alpha_2\right) = \frac{B_p}{B}\left(j_{\parallel} - j_{sat}\frac{e(\varphi - \varphi_f)}{T_e}\right) \qquad (26)$$

where $j_{sat} \sim en v_{Ti}$ is the ion saturation current, and φ_f is the floating potential. Applying the technique described in Ref. [13], one finds:

$$\dot{\xi}_{0x} = -w\left(\cos\left(\frac{\pi}{4} - \gamma\right) + \frac{R\sin\alpha_2}{x_0}\right)\frac{E\ln E}{E-1}, \quad \dot{\xi}_{0y} = -w\left(\cos\left(\frac{\pi}{4} + \gamma\right) + \frac{R\cos\alpha_2}{x_0}\right)\frac{\ln E}{E-1}, \qquad (27)$$

where the coefficient w of the dimension of velocity is defined as (Cf. [13]):

$$w = \frac{2cT_e pa^2}{B^2 j_{sat} R} \sim \mathrm{v}_{Ti} \frac{\rho_i}{R}\left(1+\frac{T_e}{T_i}\right). \tag{28}$$

We consider a filament with a circular cross-section of a radius a in the upper ("0") point.

An interesting new element compared to more qualitative discussion of Refs. [5, 19] is the appearance of the additional drive term in the y component of displacement. It is present even in the case of a zero radial tilt (α_2=0) and may cause a reversal of the normal component of the blob velocity in the upper SOL.

As was mentioned in Refs. [5,19], the length of the filament may increase because of the parallel thermal expansion of a plasma that fills it. This process is particularly important near the end nearest to the divertor plate. It may keep the blob end with contact to the plate even if the cross-field motion described by Eqs. (), () tends to move it away from the divertor plate. The relative significance of the two processes is determined by the details of the geometry. In some cases a detachment of the blob from the plate may occur, leading to a transition to the regime of accelerated motion described by Eqs. (22).

3.3 Blobs in the private flux region.

Here, again, we concentrate on the case where the plasma filament connects inner and outer divertor plates. Referring to the displacement at the inner strike point and imposing the sheath boundary at both ends, one obtains, instead of Eq. (27).

$$\dot{\xi}_{0x} = -w\left(\cos\left(\frac{\pi}{4}-\gamma\right)+\frac{R\sin\alpha_2}{x_0}-\frac{R\sin\alpha_1}{x_1}\right)\frac{E\ln E}{E-1}; \tag{29}$$

$$\dot{\xi}_{0y} = -w\left(\cos\left(\frac{\pi}{4}+\gamma\right)+\frac{R\cos\alpha_2}{y_0}-\frac{R\cos\alpha_1}{y_1}\right)\frac{\ln E}{E-1}. \tag{30}$$

Depending on the specifics of the geometry, an attachment or detachment of the blob to one or both plates may occur (see discussion at the end of Sec. 3.2).

4. Discussion

The focus of this paper was to discuss various geometrical effects that influence plasma instability and blob dynamics in the divertor region. Significant simplification in that regard comes from the fact that the magnetic field structure in the vicinity of the X-point is quite simple, and allows one to obtain very convenient mappings of the field lines. As an example of the use of these mappings, we considered plasma instabilities in the private flux region. We have managed to solve the stability problem in the realistic geometry, not in the slab model used in the earlier studies. It turned out that, in the regimes where resistive ballooning is insignificant, the growth rate reduces significantly compared to the slab approximation. This happens because the mode wave number grows significantly from the inner to the outer divertor plate. Radial tilt of the divertor plate leads to an interesting interplay of effects occurring in the inner and outer divertor legs.

We have found conditions where resistive ballooning becomes important, and decoupling of the unstable modes in the inner and the outer divertor legs occurs. This normally happens only for the modes with a small cross-field scale length. The instability in this regime is sensitive to the tilt of the divertor plates.

The shearing effect may give rise to a situation where, on the way from one divertor plate to another, the fluxtube gets sheared to the length-scale less than the ion gyroradius. In this situation, our MHD description has to be modified. The effect of the region with perturbations becoming "choppy" on the ion gyroradius scale can be accounted for by introducing an analog of the heuristic boundary condition discussed in Ref. [4]. All the rphenomena discussed would occur also in the common flux region (which we have not considered here because of the lack of space).

Our paper contains also discussion of the blob dynamics in the vicinity of the X-point. The validity of the simple model of the magnetic field used in this paper requires that the blob poloidal extension be not very large (although, on the qualitative level, our results could be used for the blobs reaching the equatorial plane). An interesting observation is that the presence of the X-point strongly affects the blob dynamics in the main SOL. So, isf one watches the blob motion in the main SOL, one can obtain a great variety of blob dynamical patterns for the blobs that look identical. This variability finds a natural explanation if one takes into account that the lower end of these blobs

can be situated at various locations with respect to the X point. Another interesting effect is that the blob extending to the divertor plate experiences a strong additional acceleration in the poloidal direction.

In all of the aforementioned problems we included one more geometrical effect, an arbitrary orientation of the separatrix quadrant with respect to the major axis (angle γ, Fig. 2).

Acknowledgment

This work was performed under the auspices of the U.S. Department of Energy by University of California Lawrence Livermore National Laboratory under contract No. W-7405-Eng-48.

References

[1] D.Farina, R.Pozzoli, D.D. Ryutov. Nucl. Fus. **33**,1315 (1993).
[2] D.Farina, R.Pozzoli, D.D. Ryutov. Plasma Phys. Contr. Fus. **35,** 1271 (1993).
[3] S.I. Krasheninnikov. Phys. Lett. **A283**, 368 (2001).
[4] D.D. Ryutov, R.H. Cohen. Contrib. Plasma Phys. **44,** 168 (2004).
[5] R.H. Cohen, et al. Nucl. Fus. **47** (2007).
[6] D.D. Ryutov, R.H. Cohen, P. Helander. Plasma Phys. Contr. Fus., **43**,1399 (2001).
[7] D.A. Russel, D. A. D'Ippolito, J.R. Myra, W.M. Nevins, X.Q. Xu. Phys.Rev. Lett., **93**, 265001 (2004).
[8] J.R. Myra, D. D'Ippolito. **12**, 92511 (2005).
[9] J.R. Myra, D.A. Russell, D.A. D'Ippolito. Phys. Plas. **13**, 112502 (2006).
[10] J.L. Terry, S.J. Zweben, K. Hallatschek, B. LaBombard, R.J. Maqueda, B. Bai, C.J. Boswell, M. Greenwald, D. Kopon, W.M. Nevins, C.S. Pitcher, B.N. Rogers, D.P. Stotler, X.Q. Xu. Phys. Plasmas, **10**, 1739 (2003).
[11] G. Grulke, J.L. Terry, B. LaBombard, S. J. Zweben. Phys. Plasmas, **13**, 012306 (2006).
[12] S.J. Zweben, R.J. Maqueda, J.L. Terry, T. Munsat, J.R. Myra, D. D'Ippolito, D.A. Russell, J.A. Krommes, B. LeBlanc, T. Stolzfus-Dueck, D.P. Stotler, K.M. Wiliams, C.E. bush, R. Maingi, O. Grulke, S.A. Sabbagh, A.E. White. Phys. Plasmas, **13**, 056114 (2006).
[13] D.D. Ryutov. Phys. Plasmas, **13**,122307 (2006).
[14] R.H.Cohen, D.D. Ryutov. Phys. Plasmas. **2**, 2011 (1995).
[15] H.Berk, D.D.Ryutov, Yu. A.Tsidulko. JETP Lett., **52**, 23 (1990).
[16] H.L. Berk, R.H. Cohen, D.D. Ryutov, Yu. A. Tsidulko, X.Xu. Nuclear Fusion, **33**, 263 (1993).
[17] B.B. Kadomtsev. In: *"Reviews of Plasma Physics,"* vol.2, M.A. Leontovich, Ed., (New York, Consultants Bureau, 1965), p. 153.
[18] W. Kunkel, J. Guillory. Proceedings of the 7th International Conference on Phenomena in Ionized Gases, Edited by B. Popovich and D. Toscic (Gradjevinska Knjiga, Belgrade, Yugoslavia, 1966) Vol. 2, p. 702.
[19] P. Stangeby. "*The plasma boundary of magnetic fusion devices."* (IoP Publishing, Bristol, 2000), p. 81.
[20]S.I. Krasheninnikov, D.D. Ryutov, G. Yu. Journal of Plasma and Fusion Research, **6**, 139 (2004).
[21] O.E. Garcia, N.H. Bian, W. Fundamentski. Phys. Plasmas, **13**, 082309 (2006).
[22] R.H. Cohen, D.D. Ryutov. Contrib. Plasm. Phys., **46,** 678 (2006).
[23] D.A. D'Ippolito, J.R. Myra, S.I. Krasheninnikov. Phys. Plasmas, **9**, 222 (2002).
[24] J.R. Myra, D.A. D'Ippolito, S.I. Krasheninnikov, G.Q. Yu. Phys. Plasmas, **11**, 4267 (2004).
[25] O.E. Garcia, N.H. Bian, V. Naulin, A.H. Nielsen, J.J. Rasmussen. Phys. Plasmas, **12**, 090701 (2005).
[26] J.R. Myra, D.A. D'Ippolito. Phys. Plasmas, **12**, 093511 (2005).
[27]G.Q. Yu, S.I. Krasheninnikov, P.N. Guzdar. Phys. Plasmas, **13**, 042508 (2006)
[28] S.I. Krasheninnikov, A.I. Smolyakov, G. Yu, T.K. Soboleva. Phys. Scr., **T124**, 13 (2006).
[29] R.H.Cohen, D.D. Ryutov. Contrib. Plasma Phys., **36**, 161 (1996).